THEORETICAL DESIGN AND BENCH VALIDATION OF AN AIR-SUCTION PRECISION SEED METERING DEVICE FOR MULTIPLE SEEDS PER HILL OF SMALL-SEED CROPS

/

小籽粒种子一穴多粒气吸式精密排种器理论设计与台架验证试验

Zhiwei WANG[1)], Naishuo WEI[1)], Deyi ZHANG[1)], Sugirbay ADILET[2)], Yanwu JIANG[1)], Jianguo ZHOU[1)], Jun CHEN[1*)]

[1)] College of Mechanical and Electronic Engineering, Northwest A&F University, Yangling, Shaanxi, 712100, China

[2)] Research School of Veterinary Medicine and Agriculture, Shakarim University, Semey 071400, Kazakhstan

** Corresponding author: Jun Chen. E-mail address: chenjun_jdxy@nwsuaf.edu.cn*

DOI: https://doi.org/10.35633/inmateh-78-83

Keywords: *Small-seed crops, Seed metering device, Multi-seed per hill, Seed suction, Seed motion trajectory*

ABSTRACT

To meet the agronomic requirements for multiple-seed-per-hill sowing of millet, broomcorn millet, and rapeseed under plastic-film mulching in Northwest China, an air-suction precision seed metering device was designed and evaluated through theoretical analysis and bench testing. The device integrates seed agitation, suction, staged cleaning, conveying, unloading, and placement, and is equipped with ten hill-forming units with a hill spacing of 16 cm. The airflow field and seed motion during operation were theoretically analyzed, and seed trajectories were captured using a 300 fps high-speed imaging system at an operating speed of 3 km/h. By adjusting the inlet negative pressure and suction-hole diameter, the preliminary stable operating ranges were determined. The results showed that the observed processes of seed agitation, adsorption, cleaning, unloading, and detachment were consistent with the proposed seed-motion model. The stable negative-pressure ranges were 0.61–3.54 kPa for millet, 0.83–4.15 kPa for broomcorn millet, and 0.74–3.59 kPa for rapeseed, while the corresponding suction-hole diameter ranges were 0.6–1.2 mm, 0.8–1.4 mm, and 0.7–1.2 mm, respectively. In 1000-hill bench tests, the qualified rates reached 90.6%, 92.7%, and 91.6% for millet, broomcorn millet, and rapeseed, respectively. These results demonstrate the feasibility of the proposed device and provide a basis for further optimization and field validation.

摘要

为满足中国西北地区谷子、糜子和油菜籽覆膜播种条件下一穴多粒播种的农艺要求，设计了一种气吸式精密排种器，通过理论分析并用台架试验对其进行了验证。该装置集搅种、吸种、清种、运种、卸种和投种于一体，周向布置 10 个成穴单元，穴距为 16 cm。对其作业过程中的气场分布和种子运动进行了理论分析，并利用 300 fps 高速摄像系统在 3km/h 作业速度下对种子运动轨迹进行了观测。通过调节吸气口负压和吸孔直径，确定了排种器的初步稳定作业参数范围。结果表明，观测到的搅种、吸附、清种、卸种和脱离过程与所建立的种子运动分析结果基本一致。谷子、糜子和油菜籽对应的稳定负压范围分别为 0.61–3.54 kPa、0.83–4.15 kPa 和 0.74–3.59 kPa，相应的吸孔直径范围分别为 0.6–1.2 mm、0.8–1.4 mm 和 0.7–1.2 mm。在 1000 穴台架试验中，谷子、糜子和油菜籽的合格率分别达到 90.6%、92.7%和 91.6%。结果表明，该排种器具有良好的应用可行性，并可为后续优化设计和田间试验提供依据。

INTRODUCTION

Millet, broomcorn millet, and rapeseed are important economic crops in Northwest China *(Lei et al., 2021)*. Owing to the mountainous and hilly terrain, low temperatures, drought, and limited rainfall in this region, plastic-film mulching is widely adopted to improve soil temperature and conserve soil moisture during crop establishment. In practical production, these small-seeded crops are commonly sown with multiple seeds per hill rather than by single-seed precision sowing, because hill-drop seeding with multiple seeds can improve emergence reliability and contribute to stable stand establishment under complex field conditions *(St Jack et al., 2013; Liu et al., 2015)*. However, the requirement of depositing several seeds within one hill while maintaining a stable hill spacing places high demands on the working performance of the seed metering device *(Wang et al., 2022)*.

In recent years, considerable progress has been made in the development of precision seed metering technologies for small and medium-sized seeds. Previous studies have focused on the structural optimization of pneumatic seed metering devices, suction-hole design, airflow characteristics, and seed-cleaning performance for crops such as rapeseed, celery, soybean, and buckwheat *(Ibrahim et al., 2018; Lei et al., 2020; Li et al., 2023; Qiao et al., 2023; Li et al., 2025)*. *Zheng et al. (2022)* pointed out that seed metering technologies are developing toward higher precision, stronger adaptability, and closer integration with agronomic requirements. Among the available approaches, air-suction seed metering devices have attracted considerable attention because they provide gentle seed handling, adjustable suction conditions, and good potential for precision hill-drop seeding.

Nevertheless, most existing studies have focused on single-seed pickup or conventional precision seeding, whereas research on air-suction seed metering devices specifically designed for multiple-seed-per-hill sowing of millet, broomcorn millet, and rapeseed under plastic-film mulching remains limited. In such an operating mode, the seed metering device must simultaneously satisfy several requirements, including stable seed agitation and filling, controlled seed pickup, effective staged seed cleaning, orderly seed conveying, and concentrated seed release within each hill *(Singh et al., 2005; Gaikwad and Sirohi, 2008)*. The coupling of these processes makes the design and theoretical analysis of the device more complex than those of conventional single-seed metering systems *(Liao et al., 2017)*. In addition, the airflow-field distribution and the motion behavior of seeds throughout the entire operating process must be clarified to provide a reliable basis for structural design and parameter selection.

Therefore, the objective of this study was to design an air-suction precision seed metering device suitable for multiple-seed-per-hill sowing of millet, broomcorn millet, and rapeseed, and to conduct a preliminary bench validation of its operating mechanism. Specifically, the overall structure and working principle of the device were analyzed, theoretical models of the airflow field and seed motion trajectory were established, and a high-speed imaging bench test was conducted to verify the seed movement process during operation. In addition, the preliminary stable ranges of inlet negative pressure and suction-hole diameter for the three seed types were determined. This study provides a theoretical and experimental basis for the subsequent optimization of the seed metering plate, seed agitation plate, seed-cleaning mechanism, and the perforating mechanism, as well as for future field performance evaluation.

MATERIAL AND METHODS

Agronomic requirements and technical parameters

As shown in Fig. 1, a schematic diagram of the typical planting agronomy for small-seed crops in northwest China is presented. Northwest China is characterized by mountainous and hilly terrain, a relatively dry climate with limited rainfall, and comparatively low temperatures in spring and autumn. Therefore, crops such as millet, broomcorn millet, and rapeseed in this region are commonly sown under plastic film mulching to satisfy the requirements for heat preservation and moisture conservation, thereby promoting crop growth *(Yang et al., 2016)*.

Because the local germination rates of millet, broomcorn millet, and rapeseed are relatively low, 3–5 seeds or even more are generally sown in each hill. The hill spacing of these three crops is generally within the range of 12–30 cm. In this study, the hill spacing was set at 16 cm, which is the most commonly adopted value in the local area *(Yu et al., 2014)*. The requirement of depositing five seeds per hill imposes higher demands on both the design and working performance of the seed metering device. Therefore, in the subsequent experimental studies, a standard of five seeds per hill was consistently adopted for all related research and tests.

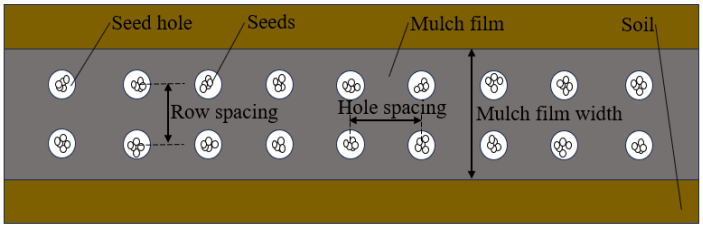

Fig. 1 - Schematic diagram of film-mulching seeding modes for small-seed crops in Northwest China

Analysis of overall structure and working principle

According to the agronomic requirements and the design principles of air-suction seed metering devices, an air-suction seed metering device suitable for multi-seed-per-hill seeding of millet, broomcorn millet, and rapeseed was designed. As shown in Fig. 2, the structural schematic of the small-seed air-suction precision seed metering device is presented. The device mainly consists of a negative-pressure air inlet, a metal shell, an air chamber housing, suction holes, a seed metering plate, a perforating mechanism, a seed-hole cleaning brush, a lower seed-cleaning knife, an upper seed-cleaning device, a seed box, and a seed unloading knife. Among these components, the seed metering plate separates the internal chamber of the seed metering device into two parts, namely the seed zone and the suction zone. Multiple groups of suction holes are arranged on a single seed metering plate, with each group corresponding to one hill. In addition, a seed agitation plate is installed on the seed metering plate, and multiple seed-agitating knobs are uniformly distributed on the agitation plate. These knobs stir the seeds accumulated in the seed zone to prevent seed piling.

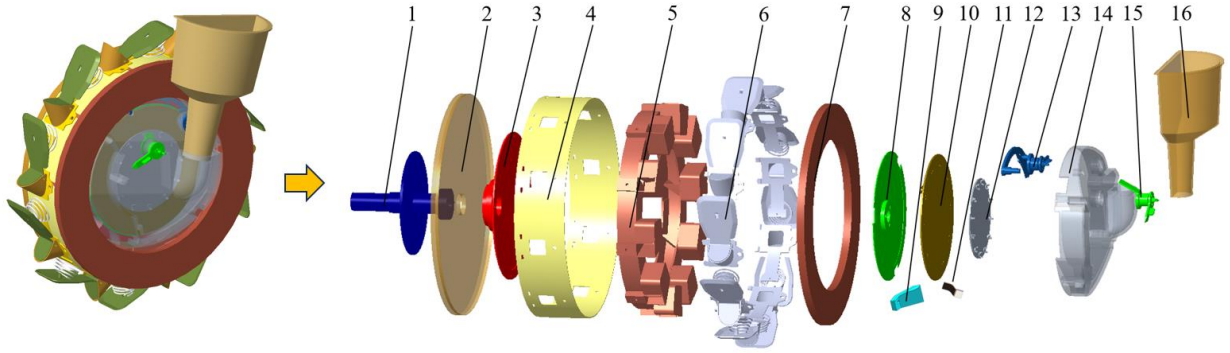

Fig. 2 - Structural schematic of the seed metering device

1. negative-pressure air inlet; 2. rear metal shell; 3. bearing turntable; 4. fixed shell; 5. seed discharge guide groove; 6. the perforating mechanism; 7. front metal shell; 8. air chamber housing; 9. seed unloading knife; 10. seed metering plate; 11. seed hole cleaning brush; 12. seed agitation plate; 13. upper seed-cleaning device; 14. seed chamber housing; 15. lower seed-cleaning knife; 16. seed box

The working process of the seed metering device mainly consists of six stages: seed agitation, seed filling, seed cleaning, seed conveying, seed unloading, and seed dropping. During seeding operation, the power source drives the fan, which is connected to the air inlet of the seed metering device through a plastic hose, thereby creating a sealed negative-pressure environment inside the suction chamber. Since the seed zone is connected to the external environment, it always remains under atmospheric pressure. When the seeds in the seed box fall into the filling area of the seed zone, they are adsorbed onto the suction holes of the seed metering plate under the action of negative pressure, thus completing the seed-filling process.

Driven by the tractor and the supporting implement, the seed metering device rotates in the circumferential direction, and the seed metering plate rotates accordingly. The seeds adsorbed on the suction holes are then carried into the seed-cleaning zone along with the rotation of the seed metering plate. Because small-seed crops have small particle sizes, multiple pickup is likely to occur under a certain level of negative pressure. When multiple pickup occurs, the combined seed-cleaning mechanism removes the excess seeds from the suction holes, thereby avoiding reseeding in each hill.

Subsequently, under the action of the negative pressure in the air chamber, the adsorbed seeds are transported over a certain distance and then enter the seed-unloading zone. At this stage, the seed-unloading knife is in close contact with the surface of the seed metering plate. When the suction holes carrying seeds move to the position where they contact the seed-unloading knife, the seeds are released from the suction holes under the lateral thrust exerted by the seed-discharge device, thereby accomplishing seed discharge. Finally, the seeds fall through the seed-guiding groove into the perforating mechanism under the action of gravity, thereby completing the seed-dropping operation.

Airflow field model and theory

Based on the analysis of the airflow field, when the seed metering plate rotates at low speed, the suction chamber can be considered a uniform pressure field, in which the pressure throughout the internal sections of the seed metering device can be approximated as uniform. In such a quasi-uniform pressure field, according to Bernoulli's equation, the pressure in the entire flow field of the seed metering device is theoretically uniform. The chamber pressure can be approximately treated as quasi-uniform on a macro scale, while local pressure gradients still exist near the suction holes *(Lei et al., 2018; Feng et al., 2023).*

As shown in Fig. 3, the airflow field of the seed metering device can be divided into three regions: the intake airflow connected to the fan, the air chamber flow field within the intake airflow, and the external flow field on the seed chamber side of the seed metering device. As illustrated, the intake pipe is connected to the electric fan via a flexible steel hose, and the seed metering plate is fixed to the rear shell of the air chamber using a clasp. During seeding operations, the seed metering plate rotates together with the main body of the seed metering device. Therefore, the air chamber distribution is circumferentially symmetric around the central axis of the intake pipe, which promotes uniformity and stability of the negative pressure field throughout the seed metering device and which simplifies theoretical analysis.

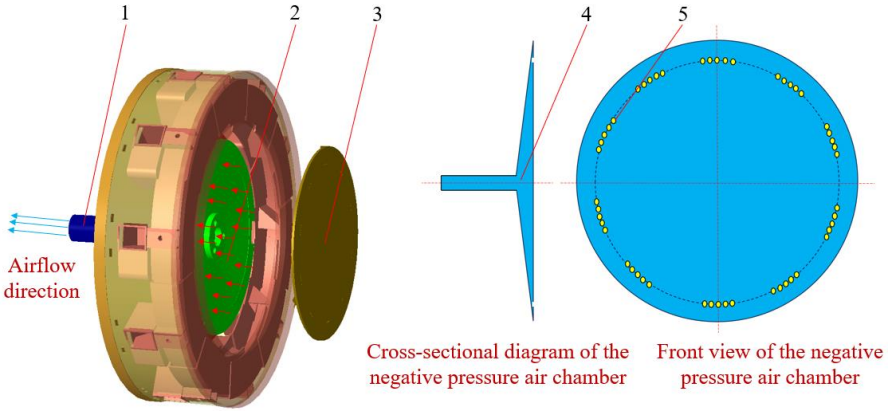

Fig. 3 - The flow field structure model of the seed metering device

1. intake pipe; 2. the rear case of air chamber; 3. Seed metering plate; 4. negative pressure chamber; 5. suction hole

The air-suction precision seed metering device uses air as the fluid medium to perform seed suction and discharge operations. Compressibility is a physical property of air as a fluid *(Xiong et al., 2021; Lu et al., 2022)*. The Mach number (M_a) is commonly used in engineering applications to represent the compressibility of a fluid. The definition of M_a is given by:

$$M_a = \frac{V}{c} = \frac{V}{\sqrt{kRT}} \quad (1)$$

where: V - air flow velocity, m/s; c - speed of sound, m/s; k - specific heat ratio, typically k=1.4 at room temperature; R - gas constant, typically R=8.314J/(mol·K); T - absolute temperature of the gas, typically T=293K at room temperature.

If air density changes are neglected, when M_a≤0.3, air can be considered incompressible. When M_a>0.3, the compressibility of air must be considered. In this study, the seeding targets are millet, broomcorn millet, and rapeseed, with an equivalent diameter range of 1.5717 mm to 2.5290 mm and 1000-seed weight ranging from 2.689 g to 8.307 g. To theoretically analyze the seed suction stage of the seed metering device, if the seed is separated from the seed cluster and can be stably attached to the suction hole, the airflow velocity at the suction hole's inlet is approximately 25.73 m/s. Substituting v=25.73 m/s (estimated based on preliminary calculations) into the Equation (1) results in:

$$M_a = 0.075 < 0.3 \quad (2)$$

From this, it can be concluded that the air in the air-suction precision seed metering device can be considered an incompressible fluid. In nature, fluid flow states can be divided into laminar flow and turbulent flow. Laminar flow refers to the flow of fluid in layers or segments, while turbulent flow includes random turbulent fluctuations superimposed on the average velocity. The Reynolds number (R_e) is used to determine whether the fluid movement is laminar or turbulent *(Xing et al., 2020)*. In engineering analysis, the critical Reynolds number is typically taken as R_e=2320 to determine the flow state. When Re≤2320, viscous forces dominate, and the flow is laminar. When R_e >2320, inertial forces dominate, and the flow is turbulent. The Reynolds number is calculated as:

$$R_e = \frac{\rho_l V L}{\mu} \quad (3)$$

where: ρ_l - air density, taken as ρ_l = 1.205 kg/m^3; V - fluid velocity, m/s; μ - fluid viscosity coefficient, for air at 25°C, μ = 1.81×10^{-5} Pa·s; L - characteristic length, for a circular pipe, L is the pipe diameter, and for non-circular pipes, L is the equivalent diameter, m.

The designed diameter of the air chamber guide slot for the air-suction seed metering device is 30 mm, so L=0.03 m. Substituting L=0.03 m and V=25.73 m/s into the Reynolds number formula:

$$R_e = 51400 > 2320 \quad (4)$$

This indicates that the Reynolds number of the airflow in the air-suction precision seed metering device's air chamber is greater than the critical value of 2320, meaning the airflow in the device is turbulent.

Analysis of seed motion trajectory

Fig. 4 shows the functional zones of the seed metering device. This zonal division provides a basis for analyzing seed motion under different operating conditions. According to the different functions of each zone during seeding, the air chamber is divided into six regions: the suction zone, transition zone, cleaning zone, conveying zone, unloading zone, and placement zone. By analyzing the forces acting on seeds in each region and considering the spatial distribution and functional characteristics of each zone, the zones are defined based on angular segmentation of the metering plate to optimize the operational performance of each part.

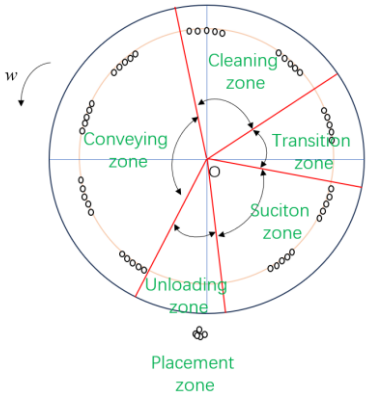

Fig. 4 - Functional zones of the seed metering device

This model serves as the foundation for subsequent analysis of seed suction, cleaning, and conveying processes. During operation in the small-seed precision seed metering device, seeds are subjected to gravitational, centrifugal, and aerodynamic forces, and their motion trajectories exhibit different motion behaviors. Therefore, establishing a theoretical model of seed motion based on the motion states of seeds in each operational stage of the seed metering device is essential for its analysis and design *(Chen et al., 2018; Sun et al., 2025).*

For simplification, seed collisions and airflow fluctuations are neglected during the operation of the seed metering device, millet, broomcorn millet, and rapeseed are approximated as spheres. The forces acting on seeds during the filling process are illustrated in Fig. 5. A seed located on the outer ring of the seed metering plate is selected as a particle, and a three-dimensional coordinate system is established. The positive (x)-axis is defined in the direction of the seed's centrifugal force, the positive (y)-axis is defined in the direction of frictional resistance between air and seed, and the positive (z)-axis is defined along the normal vector of the seed metering plate. Based on force equilibrium, the suction force required for seed attachment can be derived.

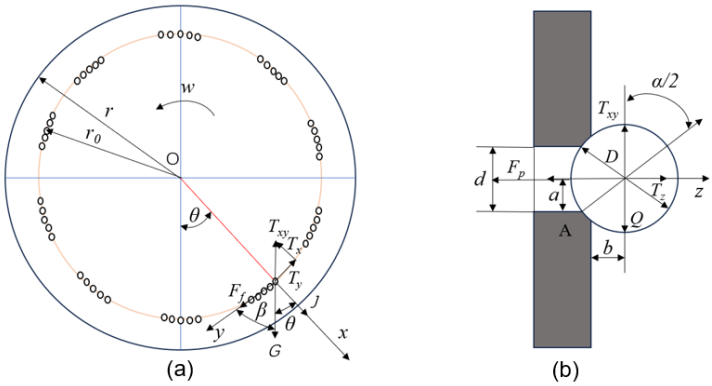

Fig. 5 - The force analysis during seed filling process

(a) The *x-y* plane force analysis; (b) The z plane force analysis

The force equilibrium equation of the seed during the filling process is expressed as follows:

$$\begin{cases} \sum F_x = 0, T_x - G\cos\theta - J = 0 \\ \sum F_y = 0, T_y - G\sin\theta - F_f = 0 \\ \sum F_z = 0, T_z - F_p = 0 \\ \sum M_A = 0, F_p a - Qb = 0 \end{cases} \quad (5)$$

where:

G - gravitational force of the seed, N; J - centrifugal force acting on the seed, N; F_f - frictional resistance between the seed and air, N; Q - resultant force of G, J, and F_f, N; T - total support force exerted by the suction hole on the seed, N; T_x - component of T along the x-axis, N; T_y - component of T along the y-axis, N; T_z - component of T along the z-axis, N; a - distance from the suction point to the axis of the suction hole, m; b - distance from the suction point to the resultant force Q, m; θ - angle between the line connecting the seed's center of gravity and the plate center and the reference direction, °.

From Equation (5), the constraint force acting on the seed during the suction process in the xy - plane can be expressed as:

$$T_{xy} = \sqrt{T_x^2 + T_y^2} = \sqrt{G^2 + J^2 + F_f + 2G\sqrt{(J^2 + F_f^2)}\sin(\theta + \beta)} \quad (6)$$

where:

β - the angle between the gravitational force and the y-axis, °; T_{xy} - the resultant force of T_x and T_y, N.

If the seed at the suction hole is in force equilibrium, then:

$$F_p = Qa/b = Q\tan\ （\alpha/2）\ = T_{xy}\tan(\alpha/2) = \sqrt{J^2 + G^2 + F_f^2 + 2G\sqrt{(J^2 + F_f^2)}\sin(\theta + \beta)} \times \tan(\alpha/2) \quad (7)$$

where:

F_p - the suction force acting on the seed, N.

The critical vacuum pressure at the suction hole P is given by:

$$P = \frac{F_p}{S} = \frac{4\sqrt{J^2 + G^2 + F_f^2 + 2G\sqrt{(J^2 + F_f^2)}\sin(\theta + \beta)} \times \sin(\alpha/2)}{\pi D^2 \cos^3(\alpha/2)} \quad (8)$$

where: P - the theoretical vacuum pressure at which the seed can be suctioned during the suction process, kPa; S - the area of the seed subjected to force at the suction hole, m².

In actual seeding operations, due to external factors such as air resistance, machine vibration, and variations in seed size, shape, and specifications, and to ensure the reliability of the seed suction process, the minimum vacuum pressure P_{0min} required for seed suction should be:

$$P_{0\min} = K_1 K_2 P = K_1 K_2 \frac{4\sqrt{J^2 + G^2 + F_f^2 + 2G\sqrt{(J^2 + F_f^2)}\sin(\theta + \beta)} \times \sin(\alpha/2)}{\pi D^2 \cos^3(\alpha/2)} \quad (9)$$

where: K_1 - external condition coefficient; K_2 - seed suction reliability coefficient.

K_1 is the external influence coefficient accounting for factors affecting the seed suction process, such as air resistance and external vibrations, typically ranging from 1.8 to 2. K_2 is the suction reliability coefficient used to compensate for errors caused by variations in seed size, shape, and inter-seed collisions, typically ranging from 1.8 to 2; here, it is taken as 2 *(Chen et al., 2018)*.

From Equation (9), the results indicate that during the suction process, the required vacuum pressure of the suction air chamber is related to factors such as the suction hole cone angle, the linear velocity of the seed, and the properties of the seed itself.

During the seed conveying process, the pressure and other environmental conditions are relatively stable. Seeds at the suction holes move in uniform circular motion with the rotation of the seed metering plate. At this stage, the forces acting on the seeds are steady, and seed–seed interactions are neglected. Therefore, the seeds can be considered unaffected by air resistance and other frictional forces, i.e., F_f was neglected for simplification under relatively stable conveying conditions. According to Equation (9), under the condition of a constant seed adhesion area, the minimum vacuum pressure required during the transport process, P_{1min}, is:

$$P_{1\min} = \frac{F_{p\min}}{S} = \frac{4(G+J)\times\sin(\alpha/2)}{\pi D^2\cos^3(\alpha/2)} \tag{10}$$

At this stage, $\theta + \beta$ = 90°. Based on the above formulas and analysis, the results indicate that in a stable and uniform airflow field, the minimum vacuum pressure required in the filling zone is much higher than that in the seed transport zone. Therefore, meeting the vacuum pressure requirement during the filling process is sufficient to satisfy the demands of the conveying process.

During the seed unloading process, seeds are affected by the air chamber vacuum, the support force of the seed metering plate, and the lateral thrust from the discharge device. Under the action of the lateral thrust, seeds detach from the seed metering plate and are released into the placement zone.

In the seed placement process, the vacuum suction force on the seeds disappears. At this point, seeds are acted upon by their own weight and air resistance and begin to follow a parabolic trajectory with a given initial velocity. The seed motion velocity is relatively low, and air resistance is neglected. A planar rectangular coordinate system is established for a single-hole seed, as shown in Fig. 6, to analyze the motion of the first and the last seeds detaching from the seed holes during the placement process.

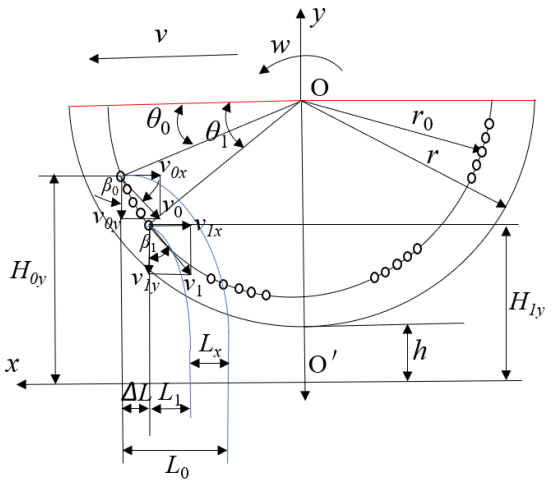

Fig. 6 - Motion analysis of seeds throwing process

Fig. 6 shows the horizontal distance difference between the first and last seeds detaching from the seed hole upon landing:

$$L_x = L_1 - (L_0 - \Delta L) = w/g \times \left\{ \begin{array}{c} r_0\sin\beta_0\left(\sqrt{w^2 r_0^2\cos^2\beta_0 + 2gH_{0y}}\right) - \\ r\sin\beta_1\left(\sqrt{w^2 r_0^1\cos^2\beta_1 + 2gH_{1y}} - wr\cos\beta_1\right) \end{array} \right\} + \Delta L \tag{11}$$

where:

v - forward velocity of the seed metering plate, m/s; θ_0 - angle between the line connecting the first seed of each hole and the plate center with the horizontal plane at the moment it leaves the plate, °; θ_1 - angle between the line connecting the last seed of each hole and the plate center with the horizontal plane at the moment it leaves the plate, °; h - distance from the lowest point of the seed metering plate to the ground, m; v_0 - velocity of the first seed leaving the plate, m/s; v_1 - velocity of the last seed leaving the plate, m/s; v_{0x} - horizontal component of the first seed's velocity, m/s; v_{0y} - vertical component of the first seed's velocity, m/s; v_{1x} - horizontal component of the last seed's velocity, m/s; v_{1y} - vertical component of the last seed's velocity, m/s; β_0 - angle between the initial velocity v_0 of the first seed and the vertical direction, °; β_1 - angle between

the initial velocity v_1 of the last seed and the vertical direction, °; H_{0y} - height of the first seed above the ground when leaving the plate, m; H_{1y} - height of the last seed above the ground when leaving the plate, m; L_x - horizontal distance difference between the first and last seeds upon landing, m; L_0 - horizontal distance of the first seed from the plate to the ground, m; L_1 - horizontal distance of the last seed from the plate to the ground, m.

The horizontal distance difference ΔL between the first and last seeds when they leave the seed metering plate for each hole is given by:

$$\Delta L = r_0 \cos\theta_0 - r\cos\theta_1 \quad (12)$$

From Equations (11) and (12), the results indicate that after the seeds detach from the suction holes, their motion trajectory mainly depends on factors such as the distribution of the suction holes, the sowing angle, and the angular velocity of the seed metering plate. According to the above formulas, when five suction holes are assigned to each seeding unit, the more compact the arrangement of the seed holes, the higher the synchronization of the seeds in each hole, resulting in a smaller placement angle, meaning the seed placement will be closer to the ground. This leads to better seed placement performance. Therefore, when selecting and designing the seed placement position, these factors and parameters should be considered as key design parameters.

Bench validation test

Based on the previous investigation of the overall structure of the small-seed air-suction precision seed metering device, a prototype of the device was developed. Optimization studies were then carried out on its major components, including the seed metering plate, seed agitation plate, seed-cleaning mechanism, and the perforating mechanism. These components will be described in detail in subsequent papers of this series.

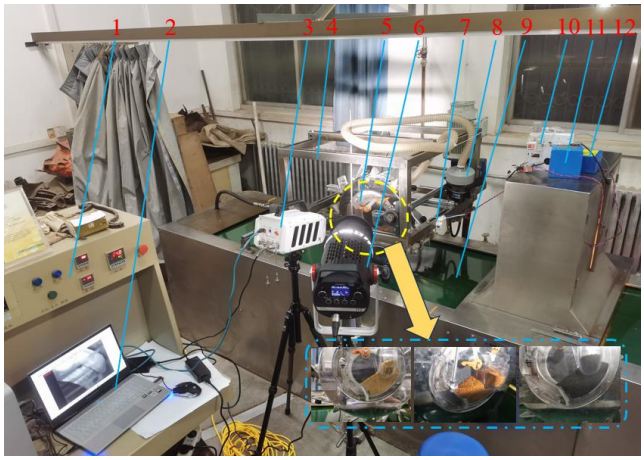

Fig. 7 - Bench test platform

1. control console, 2. laptop computer, 3. high-speed camera, 4. fixing device, 5. seed metering device, 6. lighting system, 7. fan switch, 8. negative-pressure fan, 9. conveyor belt, 10. negative-pressure regulating device, 11. power supply of the negative-pressure regulating device, 12. power supply of the negative-pressure fan

In this study, ten perforating mechanisms were uniformly arranged around the circumference of the seed metering device, corresponding to ten hills, with a hill spacing of 16 cm. To verify the correctness of the relevant theories concerning the airflow field in the seed chamber and the motion trajectories of seeds during the entire operating process of the seed metering device, a test system for the seed metering device was established. As shown in Fig. 7, the system mainly consisted of a control console, a laptop computer, a high-speed camera, a fixing device, a lighting system, a negative-pressure fan, a conveyor belt, and a negative-pressure regulating device. The high-speed imaging system used in the test was an Olympus I-speed TR high-speed camera. During the experiment, the shooting speed of the high-speed camera was set to 300 fps. After the test, the acquired images and experimental data were analyzed and processed using the supporting video post-processing software, i-SPEED Control Software.

This study was a preliminary validation test of the overall structure and theory. Since the typical operating speed of seeding on plastic film ranges from 2 to 5 km/h, the operating speed in the experiment was set at 3 km/h. By adjusting the negative pressure and the suction-hole diameter of the seed metering plate, the adsorption state and motion trajectories of the seeds were observed. The main purpose was to determine the reasonable ranges of suction-hole diameter and air-chamber negative pressure corresponding to millet, broomcorn millet, and rapeseed. In this test, the accuracy of the negative-pressure regulating device was 0.1

kPa. Stable adsorption of the seeds throughout the entire operating process and successful removal of the seeds by the seed discharge knife during the discharge process were taken as the qualification criteria.

RESULTS AND DISCUSSION

As shown in Fig. 8, the seed trajectories throughout the entire operating process of the seed metering device were observed using a high-speed imaging system. Combined with the control of negative pressure, these observations were used to verify the mathematical model for seed motion trajectory analysis. In Fig. 8(a), the seed agitation plate stirs the seed population, thereby improving seed flowability. After seeds are adsorbed by the suction holes, some excess seeds remain attached around the holes. As the seed metering plate rotates, the upper seed-cleaning device removes most of the excess seeds, as shown in Fig. 8(b). When the seed population rotates to the position of the lower seed-cleaning knife in Fig. 8(c), the knife further removes the excess seeds located below the suction holes, ensuring that only one seed is retained at each suction hole and thus guaranteeing seeding precision. As shown in Fig. 8(d)–(f), when the seed metering plate carries the seeds to the seed-release knife, the seeds are subjected to tangential force, lose the negative-pressure adsorption force at the suction holes, and fall under gravity into the seed delivery zone. The seed behavior at each stage of the metering process verified the rationality of the mathematical model for seed motion analysis.

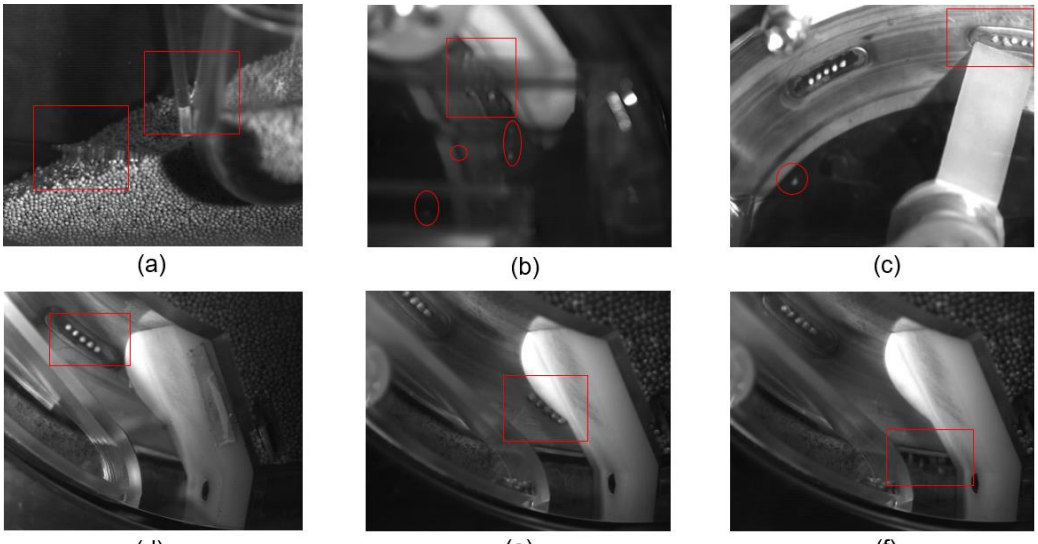

Fig. 8 - Seed motion trajectories observed by high-speed imaging during the operation of the seed metering device

(a) Seed agitation stage; (b) Upper seed-cleaning stage; (c) Lower seed-cleaning stage; (d) Stable seed adsorption stage; (e) Seed release stage; (f) Seed separation from the seed metering plate.

As shown in Table 1, the negative pressure at the air inlet of the seed metering device and the diameter of the suction holes on the seed metering plate were adjusted through bench experiments, and the preliminary stable operating parameter ranges for millet, broomcorn millet, and rapeseed were obtained. The corresponding negative pressure ranges were 0.61–3.54 kPa, 0.83–4.15 kPa, and 0.74–3.59 kPa, respectively, whereas the corresponding suction hole diameter ranges were 0.6–1.2 mm, 0.8–1.4 mm, and 0.7–1.2 mm, respectively. The results showed that the suction hole diameter increased in the order of millet, rapeseed, and broomcorn millet, and the corresponding negative pressure range exhibited the same trend, which was likely related to the increases in seed volume and mass among the three seed types.

Table 1

Preliminary stable operating parameter ranges of the seed metering device at 3 km/h

Seed type	Negative pressure range [kPa]	Suction hole diameter range [mm]
Millet	0.61-3.54	0.6-1.2
Broomcorn millet	0.83-4.15	0.8-1.4
Rapeseed	0.74-3.59	0.7-1.2

Fig. 9(a)–(c) show the seed distribution performance of millet, broomcorn millet, and rapeseed on the conveyor belt during bench tests conducted at an operating speed of 3 km/h. The results demonstrated that the seed metering device had high operational stability and could basically achieve five seeds per hill.

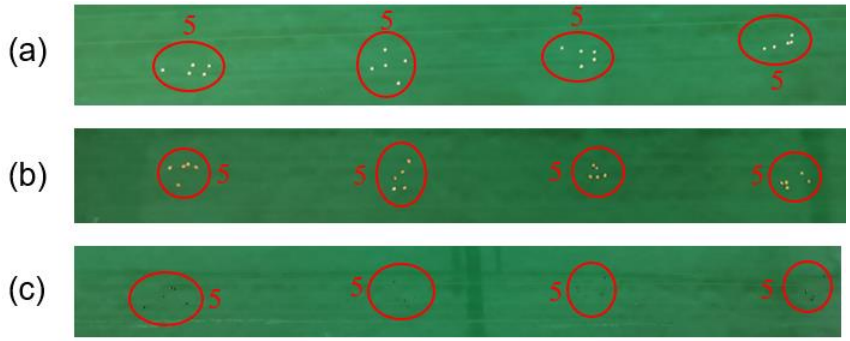

Fig. 9 - Seed metering performance in the bench test
(a) millet; (b) broomcorn millet; (c) rapeseed

To accurately evaluate the operating performance of the seed metering device, the median values of the negative pressure range and suction-hole diameter range corresponding to each seed type were selected. Specifically, the operating parameters were set as follows: for millet, a negative pressure of 2.1 kPa and a suction-hole diameter of 0.9 mm; for broomcorn millet, a negative pressure of 2.5 kPa and a suction-hole diameter of 1.1 mm; and for rapeseed, a negative pressure of 2.2 kPa and a suction-hole diameter of 1.0 mm. At an operating speed of 3 km/h, the seed metering performance of 1000 hills was recorded for each seed type. A hill with more than five seeds was defined as over-seeding, a hill with fewer than five seeds was defined as miss-seeding, and a hill with exactly five seeds was considered qualified. The results showed that the miss-seeding rate, over-seeding rate, and qualified rate were 2.3%, 7.1%, and 90.6% for millet; 3.5%, 3.8%, and 92.7% for broomcorn millet; and 1.9%, 6.5%, and 91.6% for rapeseed, respectively. These results indicate that the seed metering device exhibited high operational stability and showed promising performance with multiple small seeds per hill.

CONCLUSIONS

(1) An air-suction precision seed metering device suitable for multiple-seed-per-hill sowing of millet, broomcorn millet, and rapeseed under plastic-film mulching was designed. The device integrated seed agitation, seed suction, staged seed cleaning, seed conveying, seed unloading, and seed placement, and was configured with ten hill-forming units at a hill spacing of 16 cm.

(2) The overall structure, working principle, airflow-field characteristics, and seed motion process of the device were analyzed theoretically. The proposed models provided a basis for explaining seed filling, cleaning, conveying, unloading, and placement during operation.

(3) High-speed imaging bench tests preliminarily verified the operating process of the device. The observed seed agitation, adsorption, upper and lower seed-cleaning, seed release, and seed separation behaviors were basically consistent with the proposed seed-motion analysis.

(4) At an operating speed of 3 km/h, the preliminary stable ranges of inlet negative pressure and suction-hole diameter were 0.61–3.54 kPa and 0.6–1.2 mm for millet, 0.83–4.15 kPa and 0.8–1.4 mm for broomcorn millet, and 0.74–3.59 kPa and 0.7–1.2 mm for rapeseed, respectively.

(5) Under representative parameter combinations, the qualified rates for millet, broomcorn millet, and rapeseed were 90.6%, 92.7%, and 91.6%, respectively, indicating that the proposed device has good feasibility and operational stability for multiple-seed-per-hill seeding of small-seed crops.

ACKNOWLEDGEMENT

This study was supported by the National Natural Science Foundation of China (32272001), the Shaanxi Key Research and Development Project (2023-ZDLNY-62), and the Shaanxi Key Research and Development Project (grant number 2022NY-205).

REFERENCES

[1] Chen M., Diao P., Zhang Y., Gao Q., Yang Z., & Yao W. (2018). Design of pneumatic seed-metering device with single seed-metering plate for double-row in soybean narrow-row-dense-planting seeder (大

豆窄行密植播种机单盘双行气吸式排种器设计). *Transactions of the Chinese Society of Agricultural Engineering*, 34(21), 8-16. https://doi.org/10.11975/j.issn.1002-6819.2018.21.002

[2] Feng, D., Sun, X., Li, H., Qi, X., Wang, Y., & Nyambura, S. M. (2023). Optimized design of the pneumatic precision seed-metering device for carrots. *International Journal of Agricultural and Biological Engineering*, 16(6), 134-147. https://doi.org/10.25165/j.ijabe.20231606.7911

[3] Gaikwad B.B., & Sirohi N.P.S. (2008). Design of a low-cost pneumatic seeder for nursery plug trays. *Biosystems Engineering*, 99(3), 322-329. https://doi.org/10.1016/j.biosystemseng.2007.10.017

[4] Ibrahim, E. J., Liao, Q., Wang, L., Liao, Y., & Yao, L. (2018). Design and experiment of multi-row pneumatic precision metering device for rapeseed. *International Journal of Agricultural and Biological Engineering*, 11(5), 116-123. https://doi.org/10.25165/j.ijabe.20181105.3544

[5] Lei X., Liao Y., Zhang Q., Wang L., & Liao Q. (2018). Numerical simulation of seed motion characteristics of distribution head for rapeseed and wheat. *Computers and Electronics in Agriculture*, 150, 98-109. https://doi.org/10.1016/j.compag.2018.04.009

[6] Lei X., Yang W., Yang L., Liu L., Liao Q. & Ren W. (2020). Design and experiment of seed hill-seeding centralized metering device for rapeseed (油菜精量穴播集中排种装置设计与试验). *Transactions of the Chinese Society for Agricultural Machinery*, 51(2), 54-64. https://doi.org/10.6041/j.issn.1000-1298.2020.02.007

[7] Lei X., Hu H., Yang W., Liu L., Liao Q., & Ren W. (2021). Seeding performance of air-assisted centralized seed-metering device for rapeseed. *International Journal of Agricultural and Biological Engineering*, 14(5), 79-87. https://doi.org/10.25165/j.ijabe.20211405.5349

[8] Li H., Ma Y., Yu H., Wang Y., Sun X., & Yin J. (2023). Design and experiment of group air-suction type celery seed metering device (群组吸孔气吸式芹菜排种器设计与试验). *Transactions of the Chinese Society for Agricultural Machinery*, 54(3), 87-95. https://doi.org/10.6041/j.issn.1000-1298.2023.03.009

[9] Li Q., Xu G., & Feng J. (2025). Design and experimental of a seed metering device for small sized vegetable seeds. *INMATEH Agricultural Engineering*, 76(2), 994-1005. https://doi.org/10.35633/inmateh-76-85

[10] Liao Y., Wang L., & Liao Q. (2017). Design and test of an inside-filling pneumatic precision centralized seed-metering device for rapeseed. *International Journal of Agricultural and Biological Engineering*, 10(2), 56-62. https://doi.org/10.3965/j.ijabe.20171002.2061

[11] Liu H., Guo L., Fu L., & Tang S. (2015). Study on multi-size seed-metering device for vertical plate soybean precision planter. *International Journal of Agricultural and Biological Engineering*, 08(1), 1-8. https://doi.org/10.3965/j.ijabe.20150801.001

[12] Lu, B., Ni, X., Li, S., Li, K., & Qi, Q. (2022). Simulation and experimental study of a split high-speed precision seeding system. *Agriculture*, 12(7), 1037. https://doi.org/10.3390/agriculture12071037

[13] Qiao, X., Liu, D., Wang, X., Li, W., Wang, J., & Zheng, D. (2023). Design and experiment of double-row seed-metering device for buckwheat large ridges. *Agriculture*, 13(10), 1953. https://doi.org/10.3390/agriculture13101953

[14] Singh R.C., Singh G., & Saraswat D.C. (2005). Optimisation of design and operational parameters of a pneumatic seed metering device for planting cottonseeds. *Biosystems Engineering*, 92(4), 429-438. https://doi.org/10.1016/j.biosystemseng.2005.07.002

[15] St Jack D., Hesterman D., & Guzzomi A. (2013). Precision metering of Santalum spicatum (Australian sandalwood) seeds. Biosystems Engineering, 115(2), 171-183. https://doi.org/10.1016/j.biosystemseng.2013.03.004

[16] Sun W., Yi S, Qi H., Li Y., Dai Z., Zhang, Y., Yuan J., & Wang, S. (2025). Design and optimization of air-assisted spiral seed-supply device for high speed dense planting maize seeder. *INMATEH Agricultural Engineering*, 75(1), 13-25. https://doi.org/10.35633/inmateh-75-01

[17] Wang B., Wang L., Liao Y., Wu C., Cao M., & Liao Q. (2022). Design and test of seeding wheels of precision hole-seeding centralized metering device for small particle size seeds (小粒径种子精量穴播集排器型孔轮设计与试验).*Transactions of the Chinese Society for Agricultural Machinery*, 53(11), 64-75，119. https://doi.org/10.6041/j.issn.1000-1298.2022.11.007

[18] Xing H., Wang Z., Luo X., He S., & Zang Y. (2020). Mechanism modeling and experimental analysis of seed throwing with rice pneumatic seed metering device with adjustable seeding rate. *Computers and Electronics in Agriculture*, 178, 105697. https://doi.org/10.1016/j.compag.2020.105697

[19] Xiong, D., Wu, M., Xie, W., Liu, R., & Luo, H. (2021). Design and experimental study of the general mechanical pneumatic combined seed metering device. *Applied Sciences*, 11(16), 7223. https://doi.org/10.3390/app11167223

[20] Yang L., Yan B., Cui T., Yu Y., He X., Liu Q., Liang Z., Yin X., & Zhang D. (2016). Global overview of research progress and development of precision maize planters. *International Journal of Agricultural and Biological Engineering*, 9(1), 9-26. https://doi.org/10.3965/j.ijabe.20160901.2285

[21] Yu J., Liao Y., Cong J., Yang S., & Liao Q. (2014). Simulation analysis and match experiment on negative and positive pressures of pneumatic precision metering device for rapeseed. *International Journal of Agricultural and Biological Engineering*, 7(3), 1-12. https://doi.org/10.3965/j.ijabe.20140703.001

[22] Zheng J., Liao Y., Liao Q., & Sun M. (2022). Trend analysis and prospects of seed metering technologies (播种机排种技术研究态势分析与趋势展望). *Transactions of the Chinese Society of Agricultural Engineering*, 38(24): 1-13. https://doi.org/10.11975/j.issn.1002-6819.2022.24.001